British Geological Survey
NATURAL ENVIRONMENT RESEARCH COUNCIL

Metamorphism of the Lower Palaeozoic rocks of the Moffat district, southern Scotland, 1:50K Sheet 16W

Integrated Geoscience Surveys Northern Britain

Internal Report IR/04/120

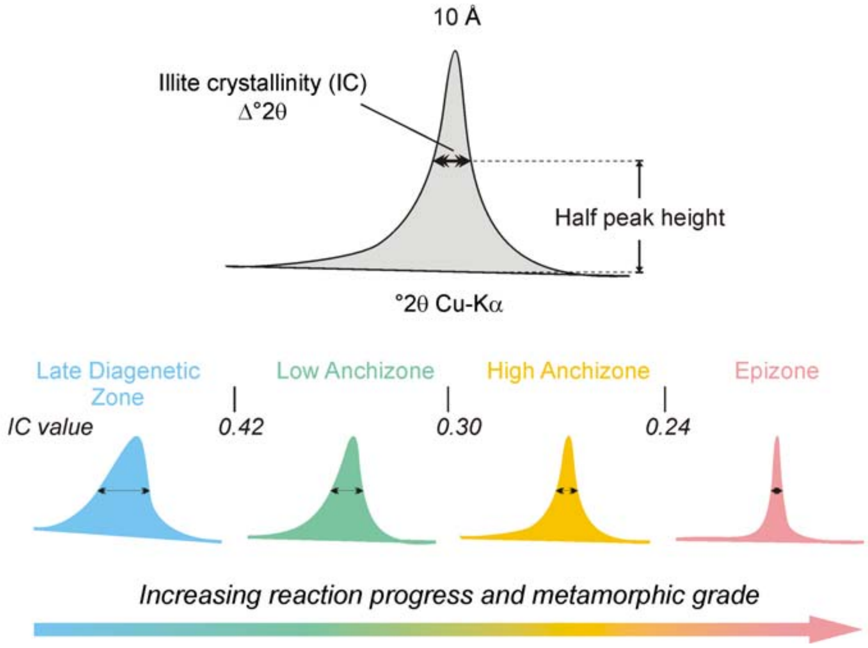

BRITISH GEOLOGICAL SURVEY

INTERNAL REPORT IR/04/120

Metamorphism of the Lower Palaeozoic rocks of the Moffat district, southern Scotland, 1:50K Sheet 16W

S J Kemp and R J Merriman

Key words

Low grade metamorphism, mica (illite) crystallinity, accretion.

Front cover

Illite crystallinity cartoon

Bibliographical reference

KEMP, S J AND MERRIMAN, R J. 2004. Metamorphism of Lower Palaeozoic rocks from the Moffat district, southern Scotland, 1:50K Sheet 16W. *British Geological Survey Internal Report*, IR/04/120. 21pp.

Keyworth, Nottingham British Geological Survey 2004

BRITISH GEOLOGICAL SURVEY

The full range of Survey publications is available from the BGS Sales Desks at Nottingham and Edinburgh; see contact details below or shop online at www.thebgs.co.uk

The London Information Office maintains a reference collection of BGS publications including maps for consultation.

The Survey publishes an annual catalogue of its maps and other publications; this catalogue is available from any of the BGS Sales Desks.

The British Geological Survey carries out the geological survey of Great Britain and Northern Ireland (the latter as an agency service for the government of Northern Ireland), and of the surrounding continental shelf, as well as its basic research projects. It also undertakes programmes of British technical aid in geology in developing countries as arranged by the Department for International Development and other agencies.

The British Geological Survey is a component body of the Natural Environment Research Council.

Keyworth, Nottingham NG12 5GG
☎ 0115-936 3241 Fax 0115-936 3488
e-mail: sales@bgs.ac.uk
www.bgs.ac.uk
Shop online at: www.thebgs.co.uk

Murchison House, West Mains Road, Edinburgh EH9 3LA
☎ 0131-667 1000 Fax 0131-668 2683
e-mail: scotsales@bgs.ac.uk

London Information Office at the Natural History Museum (Earth Galleries), Exhibition Road, South Kensington, London SW7 2DE
☎ 020-7589 4090 Fax 020-7584 8270
☎ 020-7942 5344/45 email: bgslondon@bgs.ac.uk

Forde House, Park Five Business Centre, Harrier Way, Sowton, Exeter, Devon EX2 7HU
☎ 01392-445271 Fax 01392-445371

Geological Survey of Northern Ireland, 20 College Gardens, Belfast BT9 6BS
☎ 028-9066 6595 Fax 028-9066 2835

Maclean Building, Crowmarsh Gifford, Wallingford, Oxfordshire OX10 8BB
☎ 01491-838800 Fax 01491-692345

Parent Body

Natural Environment Research Council, Polaris House, North Star Avenue, Swindon, Wiltshire SN2 1EU
☎ 01793-411500 Fax 01793-411501
www.nerc.ac.uk

Foreword

This report is the published product of a study by the British Geological Survey (BGS) and forms part of the Core Strategic (Lands and Resources) Programme.

Acknowledgements

We are grateful to Rob Barnes and Hugh Barron (both BGS) who collected some of the pelite samples and to Rob for providing a draft geological map and advice on the interpretation of the metamorphic data.

Contents

FIGURES

Summary

The pattern of regional metamorphism indicated by illite crystallinity has been used to interpret the tectonic and thermal history of the district around Moffat in southern Scotland. The recognised regional pattern, characterised by the sub-parallelism of isocrysts with strike, and by changes in grade across the strike-parallel, tract-bounding faults is not as obvious in the Moffat district as elsewhere. The accretionary burial pattern typically found in the Southern Uplands, whereby the oldest strata show a lower metamorphic grade than younger strata, is well-defined to the north of the district but difficult to discriminate in the south. Higher grade epizonal rocks to the west of the district may represent the extension of the Moniaive Shear Zone or the an area of higher strain representing upfaulted and exhumed 'roots' of the Southern Uplands. Epizonal rocks to the north are interpreted as a surface-expression of the aureole of the concealed Tweeddale batholith. The difference in metamorphic grade noted either side of the Upper Palaeozoic Moffat Basin suggests uplift and block faulting associated with basin development. The coincidence of late diagenetic grade tracts to the west of the Moffat Basin with a Bouguer anomaly indicates the presence of a thick body of relatively low density Lower Palaeozoic rocks.

1 Introduction

Systematic studies of metapelitic grade linked with the geological re-survey of the Scottish Southern Uplands have been used to generate a series of contoured metamorphic map which currently cover nearly two-thirds of the Lower Palaeozoic terrane. These studies have used X-ray diffraction (XRD) measurements of clay mineral reaction progress, particularly *white mica (illite) crystallinity (IC)*, to delineate zones of diagenesis and low-grade metamorphism in the imbricated Ordovician and Silurian strata. Although the regional pattern revealed by *metapelitic grade* shows considerable variations in metamorphic trends, patterns of grade increasing from older into younger strata suggest that accretionary burial was the main cause of regional metamorphism (Merriman & Roberts, 2001). These patterns also reflect the different levels of exhumation of the terrane, by both normal movement on reactivated thrust faults and differential block movement on north-north-west-trending faults.

During the recent re-survey of the Moffat district, metapelitic rocks representative of the main tectonostratigraphical units were collected and used to determine white mica (illite) crystallinity indices. This report gives details of the methods used and presents the results as a contoured metamorphic map which is used to interpret the metamorphic history of the district.

2 Techniques and laboratory methods

2.1 TECHNIQUES

Burial of unconsolidated clays in basinal sequences causes progressive compaction and lithification resulting in typical shale and mudstone lithologies. The clay mineral reactions that accompany lithification transform authigenic and detrital minerals, such as smectite and kaolinite, to assemblages dominated by illite and chlorite. Tectonic deformation of these pelitic lithologies results in further progressive changes in clay mineral assemblages and the development of metapelites with a *slaty cleavage microfabric*. Progress of late diagenetic and very low grade metamorphic reactions in buried and tectonized pelitic sequences can be monitored by measuring changes in the illite–muscovite (white mica) reaction series as thicker crystallites develop in response to progressive recrystallisation (Merriman *et al.*, 1990, 1995). The *Kubler index (KI in $\Delta°2\theta$)* measures small reductions in the half-height width of the mica ~10 Å X-ray diffraction (XRD) peak which occur when the crystallite population thickens. In pelitic rock sequences the Kubler index is used to define the limits of a series of metapelitic zones of very low– and low-grade metamorphism: late diagenetic zone KI>0.42; lower anchizone KI 0.30–0.42; upper anchizone KI 0.25–0.30; epizone KI<0.25 (Merriman & Peacor, 1999).

For this study, 143 metapelites were collected from within Sheet 16W. A further 124 samples from the adjacent sheets (29 from Sheet 16E to the east, 17 from Sheet 24W to the north, 50 from Sheet 15E to the west, 14 from Sheet 10W to the south, 10 from Sheet 23E to the north-west, one from Sheet 9E to the south-west, one from Sheet 10E to the south-east and two from Sheet 24E to the north-east) were also included to allow more accurate contouring of the illite crystallinity values along the margins of Sheet 16W. A sampling density of approximately 1 metapelite per 4 km^2 was therefore achieved for Sheet 16W. All samples were prepared and analysed by XRD techniques in order to determine the Kubler Index (KI) of white mica (illite) crystallinity.

2.2 SAMPLE PREPARATION

Initial sample crushing was carried out by the BGS Sample Preparation Facility, Keyworth. After removing any surface contaminants with a wire brush, a representative 50 g portion of each sample was stage-ground, using a Cr-steel tema-mill in 5 second bursts, to pass a 1 mm sieve. Care was taken to subject the sample to short bursts of milling in order to reduce the chance of over-grinding delicate *phyllosilicate* grains.

A representative 4 g portion of the crushed sample was then placed in a boiling tube and distilled water added to a predetermined level. Each sample was then shaken thoroughly, subjected to ultrasound for 5 minutes and allowed to stand for 3 hours. Where flocculation occurred, 0.5 ml of 0.1M sodium hexametaphosphate was added and the dispersion process repeated. After 3 hours, a nominal <2 μm fraction was removed and centrifuged at maximum speed for 20 minutes. The clear supernatant was then removed and the <2 μm fraction re-dispersed in ~1 ml distilled water with a glass rod and minimal ultrasound. The <2 μm fraction slurry was then pipetted onto the surface of a frosted glass slip and allowed to dry overnight at room temperature.

2.3 X-RAY DIFFRACTION ANALYSIS

Each glass slip was analysed using a Philips PW1130 series diffractometer equipped with Ni-filtered Cu-Kα radiation and operating at 40kV and 30mA. The KIs of the samples were calculated from the mean of five scans over the range 7.5-10.5 °2θ at a speed of 0.5 °2θ/minute using the machine conditions recommended by Kisch (1991). The width of the ~10 Å peak at half-height was measured using the graphics package within PANalytical's X'Pert software suite and values were corrected using the standards of Warr & Rice (1994) to concur with measurements carried out at Birkbeck College, University of London.

A summary of sample numbers, locations and KIs are shown in the Appendix of this report. A map showing the sample locations and KI values is shown in Figure 1.

3 Lithological impacts on Kubler indices

The pelite samples collected for this study represent different lithofacies. Most of the samples were taken from the sandstone sequence and will therefore contain a variable sand/silt content while others were collected from the Moffat Shale Group which is more uniformly muddy but with possible volcanic ash input. In order to study the effect of lithofacies on the Kubler index, a small number of sample pairs were collected from approximately similar localities but representing the different lithofacies (GY1040 mudstone and GY1041 siltstone; GY1044 mudstone and GY1045 siltstone; GY1065 mudstone and GY1066 siltstone all from the Queensbury Formation; GY1047 mudstone and GY1048 siltstone from the boundary between the Selcoth and Queensbury formations).

The KI values determined for the sample pairs present apparently conflicting trends. In two pairs of samples, the mudstones (GY1047 0.38 and GY1065 0.59) were at significantly lower grade than their counterpart siltstones (GY1048 0.33 and GY1066 0.51). However in another pair of samples, the mudstone (GY1044 0.29) is at higher grade than the siltstone (GY1045 0.35) while the final pair produced very similar values (GY1040 0.27 and GY1041 0.28).

A larger study, involving a greater number of sample pairs representing a range of grades is therefore required before any conclusions may be drawn as to the effect of lithofacies on the Kubler index.

4 Metamorphic map

The metamorphic map shown in Figure 2 is the result of a computer-contoured plot of KI data, manually modified to reflect the influence of localized post–regional metamorphic events. A computer contoured geographical distribution of KI datapoints was initially produced using DeltaGraph 5.4 for Windows software. The pattern was then superimposed on an outline 1:50k geological map of the Lower Palaeozoic strata and contours redrawn where post–metamorphic faulting appeared to modify the overall pattern. In the final version of the map shown in Figure 2, contours of equal crystallinity (isocrysts) are used to delineate four metapelitic zones: late diagenetic zone (KI >0.42); lower anchizone (KI 0.30–0.42); upper anchizone (KI 0.24–0.30) and epizone (KI <0.24). In order to link with published maps for adjacent sheets the intervals used differ slightly from those described in section 2. The errors and precision involved in contouring the crystallinity data (Robinson *et al.*, 1990), were previously determined by multi–sampling at several sites in the Southern Uplands (Merriman & Roberts, 1992), and elsewhere (Roberts *et al*., 1990). The results from multi–sampled sites indicate that 95% of the samples have indices within the range of values delineated by zonal isocrysts.

The contoured metamorphic map shows a regional pattern that has a strong north-north-easterly grain. This differs from the more typical sub-parallelism of isocrysts with the regional strike and changes in grade across the strike-parallel, tract-bounding faults observed across much of the Southern Uplands terrane (Merriman & Roberts, 2001).

The oldest strata, cropping out in the north-west of the district, includes parts of the Moffat Shale Group, Crawford Group and younger Leadhills Supergroup (Kirkcolm and Portpatrick formations) and is predominantly of low anchizonal grade. A few zones of late diagenetic strata appear to represent the easterly conclusion of the complex Leadhills Imbricate Zone. The low grade of these rocks appears at odds with their burial and tectonic history but may result from retrogression due to fluid movement associated with tectonism.

The upper part of the Leadhills Supergroup (Shinnel Formation) and the lower part of the Gala Group (Mindork Formation) present higher grades – typically high anchizone but with significant areas of epizonal grade to the west and north of the district. A pattern of increasing grade from older into younger rocks between the Southern Upland Fault (to the north of the Sheet) and the Orlock Bridge Fault, is typical of the region (e.g. Kemp & Merriman, 2001). The increase in grade from the Kirkcolm to the Mindork formations is clearly shown in the lower part of Figure 3.

The western epizonal area may represent a continuation of a high grade zone on the upthrown side of the Durisdeer Fault Zone (Kemp & Merriman, 2001) attributed to the Moniaive Shear Zone (MSZ) or alternatively an area of higher strain representing upfaulted and exhumed underplated rocks of the Southern Uplands. South-east of the MSZ, grade decreases into sequentially younger rocks. The local pattern of metamorphism adjacent to the epizonal rocks of the MSZ is similar to that shown in the Leadhills district (Kemp & Merriman, 2001) but differs from that found around Moniaive, on Sheet 9W (British Geological Survey, 1998). In the Moffat and Leadhills districts, between the Upper Palaeozoic Thornhill and Moffat basins, relatively high grade (high-anchizone) rocks are found to the north-west of the MSZ, whereas around Moniaive up to 4 km of downthrow on the Orlock Bridge Fault has juxtaposed late diagenetic grade strata against the epizonal rocks of the MSZ (McMillan, 2002; Merriman & Roberts, 2001). Such differences suggest that post-shearing downthrow on the Orlock Bridge Fault was locally less than 1 km, and that to the north-east of the Thornhill Basin the Orlock Bridge Fault is inclined to the north-west, in contrast to its steep or vertical attitude in the south-west of the terrane (Barnes *et al.*, 1995; Merriman & Roberts, 2001).

The northern epizonal area, which extends northwards onto Sheet 24W, coincides with a Bouguer gravity anomaly low (Figure 2) and appears to represent the cryptic aureole of a concealed intrusion referred to as the Tweeddale Batholith (Lagios & Hipkin, 1979, 1982).

On passing into upper Gala Group and lower Hawick Group strata in the south of the district, a noticeable change in grade is apparent across the Upper Palaeozoic Moffat Basin. Predominantly late diagenetic- and low anchizonal-grade tracts to the west of the Moffat Basin are replaced by predominantly high anchizonal tracts to the east. Slivers of higher-grade epizonal strata are also exposed immediately to the east of the Moffat Basin. This interesting dichotomy is illustrated in Figure 3, by the division of the Queensberry Formation data which forms the majority of this area, into west and east subsets. The eastern subset has an average KI of 0.30 (high anchizone) while the western subset has an average KI of 0.38 (low anchizone). South of the Moffat Valley Fault, grade is similarly lower to the west of the Moffat Basin than it is to the east. The presence of major north-northwest-trending faults associated with the development of the Moffat Basin and different levels of exhumation appear to be responsible for these differences in grade on either side of the basin.

Kimbell (*pers. comm.*), however, suggests that the Moffat Basin is a relatively weak structure compared to the Lochmaben Basin to the south, perhaps because a Gala/Hawick structure acted as a transfer between the Dumfries/Lochmaben basins in the south and the Stranraer/Portpatrick basins in the north. He therefore suggests that any movement on the Moffat Basin faults was limited. Interestingly, the area of low grade rocks to the west of the Moffat Basin coincides with an along-strike termination of the Bouguer gravity density anomaly. Such changes in gravity may reflect lateral density variations within the exposed rocks or alternatively the presence of plutons or relatively dense concealed basement. New laboratory density measurements (mainly sandstones) from more than 50 sites spanning the gravity feature, combined with previous density measurements suggest the anomaly relates to a thick body of relatively low density Lower Palaeozoic rocks.

Grade appears to generally decrease to the low anchizone zone on passing into younger Hawick Group strata (Glendearg and Eskdalemuir formations) to the east of the Moffat Basin.

5 Metamorphic history

The pattern of regional metamorphism developed in the Lower Palaeozoic rocks of the Moffat district can be interpreted in terms of four tectonometamorphic events that have contributed to the evolution of the Southern Uplands terrane (Merriman & Roberts, 2001):

1. Regional very low-grade metamorphism resulting from accretionary burial
2. Possible localized shear zone metamorphism associated with the MSZ
3. Contact metamorphism associated with late, concealed granitic intrusions
4. Uplift and block faulting prior to Permo-Carboniferous basin development

Evidence for accretionary burial is difficult to discriminate in the Moffat area, as most of the district is covered by rocks of either low- or high-anchizonal grade and due to the large-scale influence of later uplift and faulting. Support for this model is most compelling in the north of the district where the older part of the Leadhills Supergroup (Kirkcolm Formation), exposed in the Leadhills Imbricate Zone, shows tracts of late diagenetic and low-anchizonal grade rocks. The younger, upper Leadhills Supergroup and lower Gala Group strata show evidence for increased burial to predominantly high-anchizonal grades (Figure 3). Similar relationships have been recorded in the Ordovician strata forming the Northern Belt (Merriman & Roberts, 1992; Stone, 1995; Hirons *et al*, 1997). Such patterns indicate that younger strata was buried beneath the older strata and in turn this suggests that the metamorphic pattern was generated by accretionary tectonism (Merriman & Roberts, 2001).

Shear-zone metamorphism associated with the MSZ may be responsible for the epizonal-grade rocks to the west of the district, straddling the Sandhead Fault. The trend of this zone of epizonal-grade rocks suggests that the MSZ swings noticeably to the north-east in the Moffat district compared to the north-north-easterly trend on the neighbouring Sheet 15E (Kemp & Merriman, 2001). As noted on Sheet 15E (Leadhills), limited downthrow (<1 km) on the Orlock Bridge Fault has preserved high-anchizonal and epizonal rocks to the north-west, that originally formed the footwall of the fault. Elsewhere, a larger downthrow on the Orlock Bridge Fault juxtaposes lower grade rocks with the MSZ.

The area of epizonal-grade rocks in the north of the district is thought to indicate the thermal aureole of a concealed, late granitic intrusion – the Tweeddale Batholith (Lagios & Hipkin, 1979, 1982). This aureole overprints the regional pattern in the Leadhills Supergroup and Gala Group. Similar late, granitic intrusions such as the Spango Pluton and Ballencleuch Law Dyke found to the west of the Moffat district, were probably generated during emplacement at depths of 6-8 km in the upper level of the Southern Uplands thrust stack (Merriman & Roberts, 2001).

Post-metamorphic uplift of the terrane led to localised reactivation of thrusts as normal faults and also to block movement along north-north-west-trending faults. Movement on both sets of faults is responsible for the present pattern of metamorphism and also the development of the half-graben Moffat Basin. The contrast in grade across the Moffat Basin is due to differential block movement which has exhumed the upper and lower levels of accreted strata comprising the Southern Uplands thrust stack. Downthrow to the west of the fault zone has preserved the lower grade strata that originally formed the upper level of the Southern Uplands thrust stack. To the east of the fault zone, higher grade rocks represent the deeper underplated level of the thrust stack.

The north-northeast trend of the low/high anchizonal boundary in both the east and west-central parts of the district are interesting. In both cases the boundary appears to cross many strike-parallel, tract-bounding faults without significant effect.

6 References

Most of the references listed below are held in the Library of the British Geological Survey at Keyworth, Nottingham. Copies of the references may be purchased from the Library subject to the current copyright legislation.

HIRONS, S R, ROBERTS, B and MERRIMAN, R J. 1997. Metamorphism of the Lower Palaeozoic rocks of the Carrick–Loch Doon region, southern Scotland. *British Geological Survey Technical Report*, WG/97/25.

KEMP, S J and MERRIMAN, R J. 2001. Metamorphism of the Lower Palaeozoic rocks of the Leadhills district, southern Scotland, 1:50K Sheets 15E and 23E. *British Geological Survey Technical Report*, IR/01/099.

KISCH, H J. 1991. Illite crystallinity: recommendations on sample preparation, X-ray diffraction settings and interlaboratory standards. *Journal of Metamorphic Geology*, 9, 665-670.

LAGIOS, E and HIPKIN, R G. 1979. The Tweeddale Granite - a newly discovered batholith in the Southern Uplands. *Nature*, 280, 672-675.

LAGIOS, E and HIPKIN, R G. 1982. A geophysical approach to the granite batholith under the eastern Southern Uplands. *Pure and Applied Geophysics*, 120, 375-388.

MERRIMAN, R J and ROBERTS, B. 1992. The low grade metamorphism of Lower Palaeozoic strata on the Rhins of Galloway, SW Scotland. *British Geological Survey Technical Report,* WG/92/40.

MERRIMAN, R J and PEACOR, D R. 1999. Very low–grade metapelites: mineralogy, microfabrics and measuring reaction progress. 10-60 in *Low–grade Metamorphism.* FREY, M and ROBINSON, D. (editors). Blackwell Science.

MERRIMAN, R J and ROBERTS, B. 2001 (for 2000). Low-grade metamorphism in the Scottish Southern Uplands terrane: deciphering the patterns of accretionary burial, shearing and cryptic aureoles. *Transactions of the Royal Society of Edinburgh: Earth Sciences*, 91, 521-537.

MERRIMAN, R J, ROBERTS, B. and PEACOR, D R. 1990. A transmission electron microscope study of white mica crystallite size distribution in a mudstone to slate transitional sequence, North Wales, U K. *Contributions to Mineralogy and Petrology*, 10**,** 27-40.

MERRIMAN, R J, ROBERTS, B, PEACOR, D R and HIRONS, S R. 1995. Strain–related differences in the crystal growth of white mica and chlorite: a TEM and XRD study of the development of metapelitic microfabrics in the Southern Uplands thrust terrane, Scotland. *Journal of Metamorphic Geology*, 13, 559–576.

ROBERTS, B, MORRISON, C and HIRONS, S R. 1990. Low grade metamorphism of the Manx Group, Isle of Man: a comparative study of white mica ‘crystallinity’ techniques. *Journal of the Geological Society of London*, 147, 271-277.

ROBERTS, B, MERRIMAN, R J and PRATT, W. 1991. The influence of strain, lithology and stratigraphical depth on white mica (illite) crystallinity in mudrocks from the vicinity of the Corris Slate Belt, Wales: implications for the timing of metamorphism in the Welsh Basin. *Geological Magazine*, 128**,** 633-645.

ROBINSON, D, WARR, L and BEVINS, R E. 1990. The illite ‘crystallinity’ technique: a critical appraisal of its precision. *Journal of Metamorphic Geology*, 8, 333-344.

STONE, P. 1995. The Geology of the Rhins of Galloway District. *Memoir of the British Geological Survey,* Sheets 1and 3 (Scotland).

WARR, L and RICE, A H N. 1994. Interlaboratory standardization and calibration of clay mineral crystallinity and crystallite size data. *Journal of Metamorphic Geology*, 12, 141–152.

Glossary

Illite crystallinity (IC) Variations in the crystallite size and lattice strain in dioctahedral mica produced in the smectite-I/S-illite-muscovite reaction series, as indicated by the Kubler index.

Kubler index (KI) The width of the X-ray diffraction c.10Å peak at half-height above background, measured as small changes in the Bragg angle $\Delta°2\theta$.

Metapelitic grade The grade of diagenesis and low-grade metamorphism indicated by reaction progress in clay minerals and other phyllosilicates.

Slaty cleavage microfabric A pervasive planar fabric consisting of submicron-spaced domains of phyllosilicates. Strain-related crystal growth of the phyllosilicates has resulted in their (00l) crystallographic planes being orientated approximately parallel to the fabric. Although the mineral constituents of the microfabric cannot be resolved with the naked eye, their parallel orientation gives rise to a fissility that dominates all other fabric elements of the mudrock and can be exploited to cleave the rock into thin (<10 mm) parallel-sided slates.

Strain-related crystal growth The crystal growth of minerals induced by rock deformation. Strain-related crystal growth is response to several interactive processes, including mechanical grain rotation of existing minerals, pressure-solution (dissolution) recrystallization and grain-boundary migration (dislocation creep) in newly-formed minerals.

Phyllosilicates A group of silicate minerals, including the micas and clay minerals, which consist of SiO_4 tetrahedra linked into flat sheets with an Si:O ratio of 1:5. Cations and water are accommodated between the sheets and such minerals are characterised by a very prominent cleavage parallel to the sheet structure.

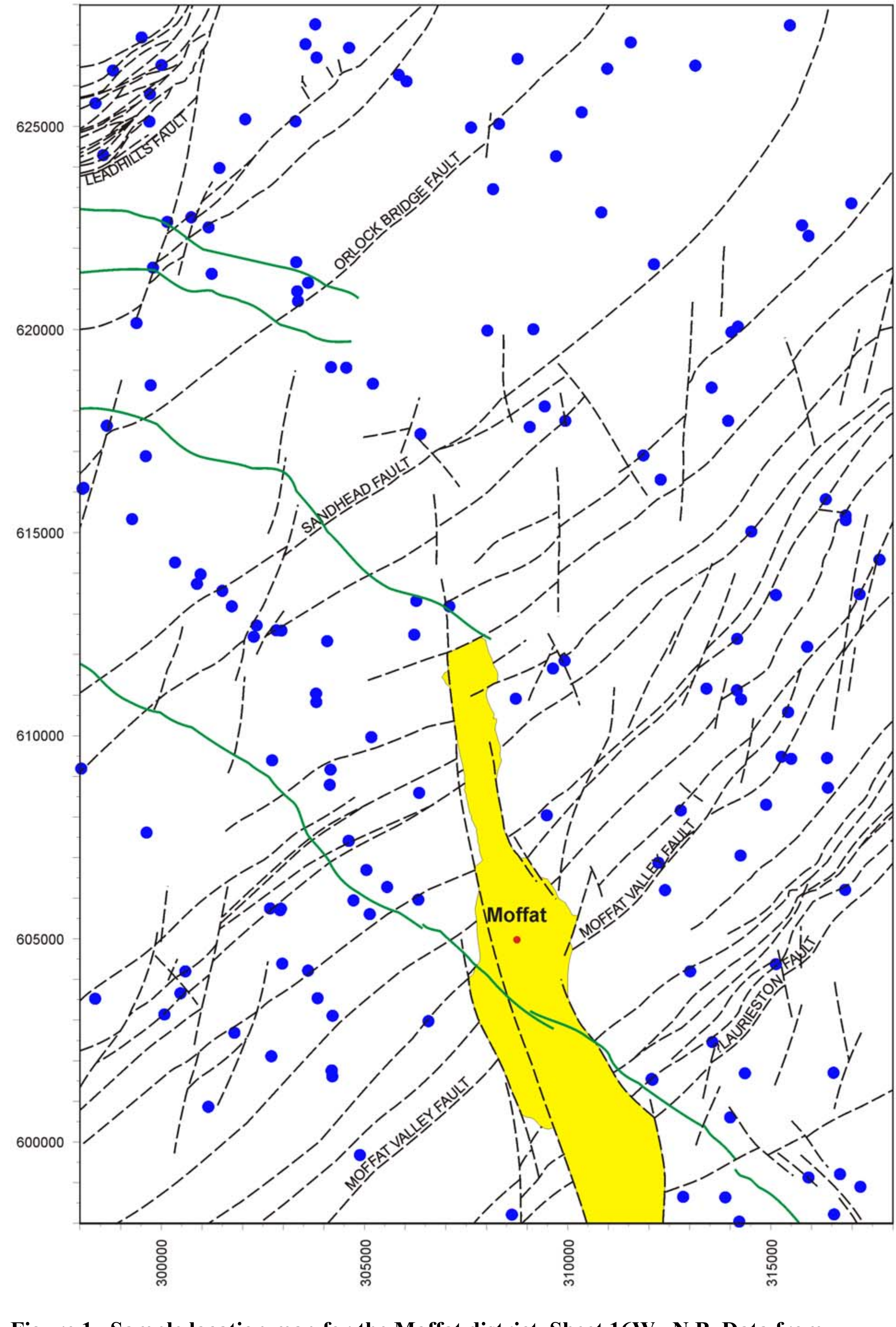

Figure 1. Sample location map for the Moffat district, Sheet 16W. N.B. Data from neighbouring sheets has been omitted.

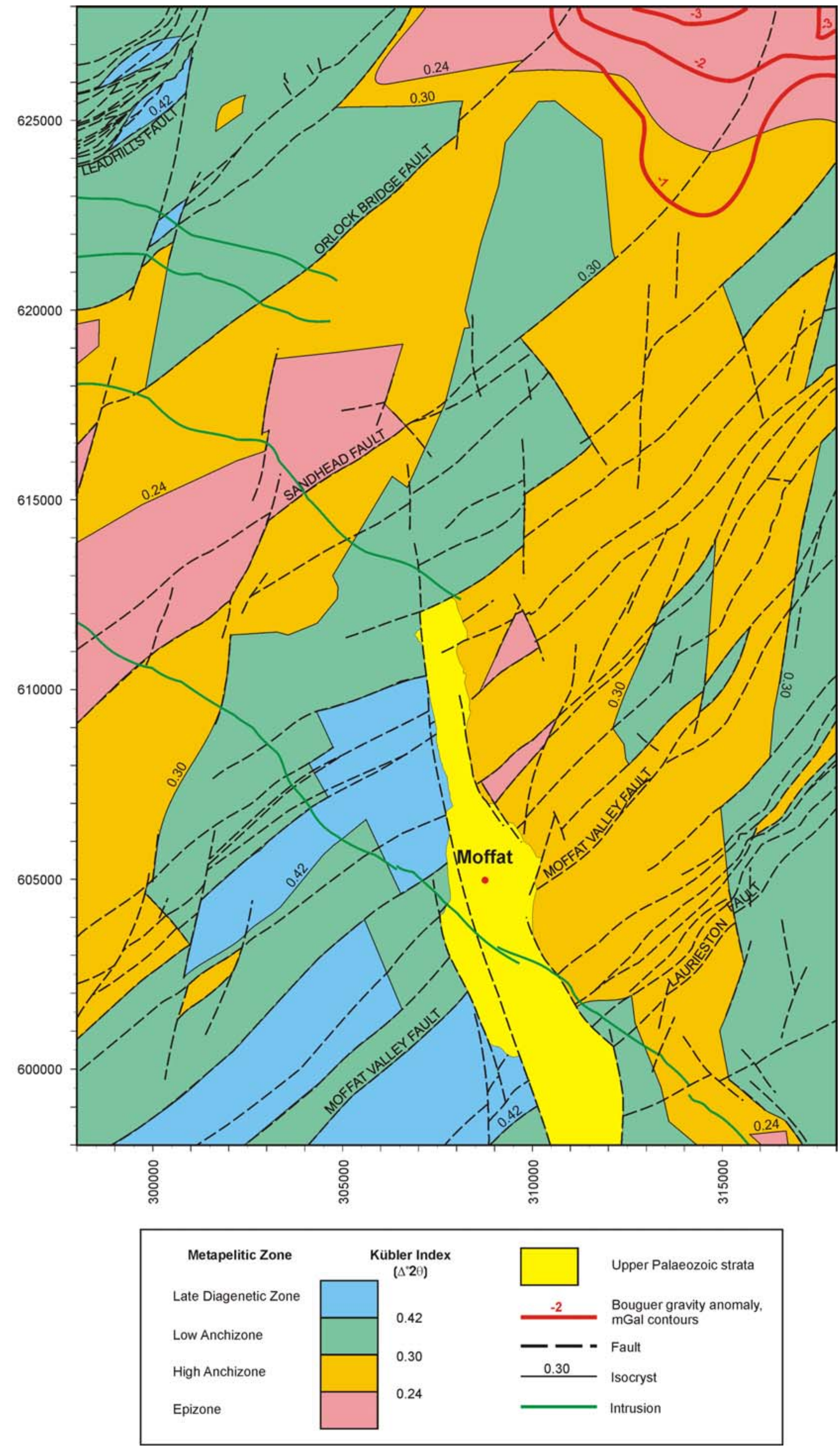

Figure 2. Contoured metamorphic map of white mica crystallinity (Kubler) indices for the Moffat district, Sheet 16W.

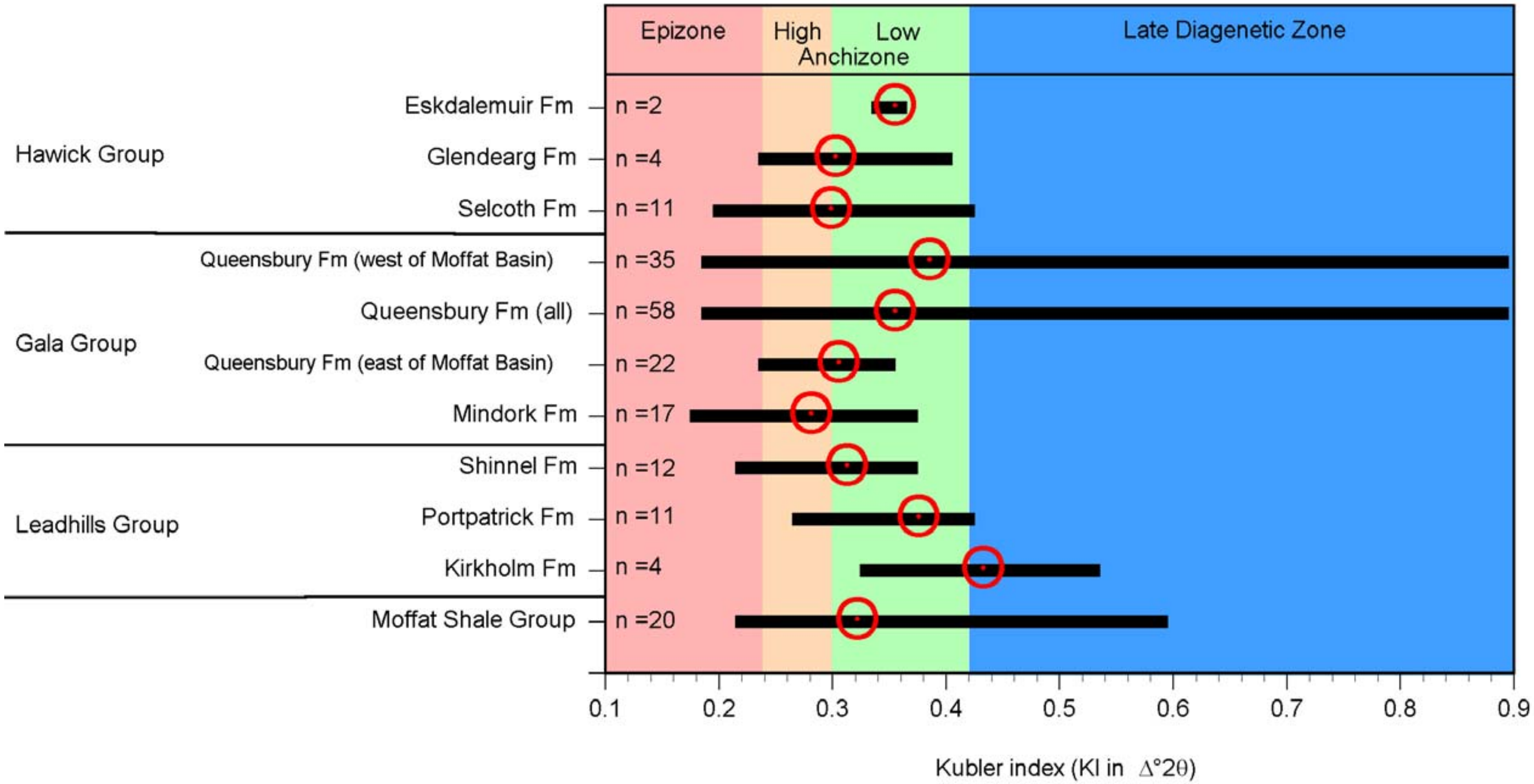

Figure 3. Stratigraphic distribution of Kubler indices for pelites from the Moffat district. Mean values are shown by ⊙.

Appendix 1 Summary of sample numbers, sample locations and KIs

1. Sheet 16W samples (m = mudstone, s = siltstone in colour-coded, matched sample pairs)

Sample No.	Square	Easting	Northing	IC
10	NT	305180	618690	0.21
11	NT	306200	612500	0.35
14	NT	314860	608310	0.25
9	NT	314500	615040	0.26
BRS997	NT	312040	601550	0.42
BRS1085	NT	316520	601700	0.4
BRS1086	NT	316680	599200	0.36
BRS1087	NT	315900	599120	0.34
GY1001	NT	312060	601530	0.33
GY1005	NT	313540	602460	0.25
GY1006	NT	309460	608050	0.20
GY1009	NT	312370	606200	0.26
GY1011	NT	312210	606880	0.27
GY1014	NT	312760	608170	0.31
GY1015	NT	312990	604200	0.28
GY1016	NT	315100	604380	0.28
GY1017	NT	312040	601550	0.42
GY1023	NT	314240	610900	0.33
GY1024	NT	314140	611130	0.36
GY1025	NT	314150	612400	0.32
GY1027	NT	305105	605611	0.33
GY1029	NT	302900	605710	0.47
GY1035	NT	300560	604200	0.33
GY1036	NT	300050	603140	0.24
GY1037	NT	306550	602970	0.30
GY1038	NT	300440	603660	0.28
GY1039	NT	315870	612200	0.27
GY1040m	NT	315100	613480	0.27
GY1041s	NT	315100	613480	0.28
GY1042	NT	304180	601610	0.89
GY1044m	NT	316820	615320	0.29
GY1045s	NT	316820	615440	0.35
GY1046	NT	316330	615840	0.24
GY1047m	NT	317160	613500	0.38
GY1048s	NT	317160	613500	0.33
GY1049	NT	315400	610590	0.30
GY1058	NT	300940	613990	0.18
GY1059	NT	301470	613580	0.19
GY1060	NT	302320	612730	0.25
GY1061	NT	302930	612600	0.24
GY1062	NT	303790	610840	0.35
GY1063	NT	304140	609170	0.35
GY1064	NT	304580	607420	0.41
GY1065m	NT	304590	607420	0.59

Sample No.	Square	Easting	Northing	IC
GY1066s	NT	305020	606700	0.51
GY1096	NT	306250	613330	0.35
GY1097	NT	307060	613200	0.34
GY1098	NT	308700	610920	0.27
GY1099	NT	309900	611860	0.27
GY1100	NT	314010	619960	0.51
GY1101	NT	313390	611170	0.31
GY1102	NT	317650	614350	0.39
GY1107	NT	309616	611669	0.22
GY1111(3)	NT	314500	615040	0.27
GY1112(4)	NT	315240	609490	0.24
GY1113(5)	NT	315480	609440	0.29
GY1114(12)	NT	316360	609460	0.30
GY1115(13)	NT	316380	608730	0.32
GY1138	NT	316806	606211	0.40
GY1142	NT	314232	607057	0.26
GY1165	NT	313852	598629	0.28
GY1166	NT	314337	601688	0.27
GY1169	NT	313979	600598	0.24
HFB141	NS	299690	625830	0.35
HFB142	NS	299680	625150	0.50
HFB143	NS	299980	626540	0.53
HFB144	NS	299490	627220	0.33
HFB235	NS	299360	620180	0.26
HFB237	NS	299710	618650	0.27
HFB250	NS	299590	616900	0.27
HFB251	NS	298630	617650	0.27
HFB261	NS	299770	621550	0.38
RJM1058	NT	303796	626725	0.36
RJM1059	NT	303523	627054	0.40
RJM618	NS	299610	607620	0.26
RJM644	NS	299250	615350	0.28
RJM695	NT	300850	613750	0.23
RJM696	NT	302250	612450	0.26
RJM697	NT	302700	609400	0.35
RJM698	NT	302650	605750	0.36
RJM699	NT	304700	605950	0.44
RJM700	NT	300310	614280	0.19
RJM701	NT	301710	613200	0.23
RJM702	NT	302800	612610	0.27
RJM703	NT	303780	611050	0.32
RJM704	NT	304120	608800	0.32
RJM705	NT	305530	606280	0.39
RJM706	NT	306300	605970	0.49

1. Sheet 16W samples (continued)

Sample No.	Square	Easting	Northing	IC
RJM707	NT	306320	608600	0.63
RJM733	NT	309690	624300	0.32
RJM734	NT	310800	622910	0.37
RJM831	NT	310320	625380	0.31
RJM832	NT	308000	620000	0.29
RJM833	NT	309130	620030	0.34
RJM834	NT	312100	621630	0.30
RJM835	NT	308140	623480	0.26
RJM836	NT	301214	621394	0.32
RJM837	NT	303333	620720	0.37
RJM838	NT	303583	621177	0.36
RJM839	NT	303319	620965	0.35
RJM840	NT	303294	621680	0.35
RJM841	NT	301135	622543	0.30
RJM842	NT	301403	624005	0.36
RJM843	NT	302040	625205	0.27
RJM844	NT	303270	625153	0.39
RJM845	NT	300712	622792	0.42
RJM846	NT	300117	622676	0.37
RJM847	NT	305140	609975	0.39
RJM848	NT	304057	612339	0.27
RJM849	NT	304527	619082	0.27
RJM850	NT	306350	617450	0.26
RJM851	NT	304147	619095	0.33
RJM852	NT	312264	616320	0.30
RJM853	NT	311840	616920	0.27
RJM854	NT	309920	617770	0.34
RJM855	NT	309040	617620	0.34

Sample No.	Square	Easting	Northing	IC
RJM856	NT	309410	618130	0.33
RJM857	NT	313926	617771	0.29
RJM858	NT	313515	618594	0.29
RJM859	NT	314169	620094	0.27
RJM864	NT	311530	627104	0.24
RJM865	NT	313115	626532	0.21
RJM866	NT	308744	626694	0.24
RJM867	NT	308285	625090	0.30
RJM868	NT	307600	625000	0.35
RJM869	NT	304170	601755	0.32
RJM870	NT	304162	601753	0.48
RJM871	NT	303816	603540	0.40
RJM872	NT	303584	604216	0.33
RJM873	NT	302949	604391	0.61
RJM874	NT	304189	603108	0.43
RJM875	NT	302678	602110	0.27
RJM876	NT	301772	602687	0.26
RJM877	NT	301127	600859	0.38
RJM878	NY	304861	599669	0.38
RJM879	NT	302918	605742	0.45
RJM880	NT	303763	627548	0.41
RJM881	NT	305813	626303	0.33
RJM882	NT	306005	626143	0.22
RJM883	NT	304596	626969	0.42
RJM890	NT	315747	622591	0.26
RJM891	NT	316960	623130	0.26
RJM892	NT	315903	622333	0.28

2. Sheet 16E samples

Sample No.	Square	Easting	Northing	IC
BRS1154	NT	318680	627400	0.33
BRS1156	NT	319910	626820	0.29
BRS1157	NT	319850	626700	0.31
GY1020	NT	318160	608900	0.27
GY1116(6)	NT	320840	622700	0.23
GY1117(7)	NT	322710	623650	0.42
GY1118(8)	NT	322050	616550	0.31
GY1119	NT	326688	614538	0.34
GY1120	NT	326701	614596	0.42
GY1123	NT	324641	614609	0.27
GY1124	NT	324366	615696	0.43
GY1126	NT	324208	615723	0.38
GY1128	NT	325490	614364	0.35
GY1131	NT	322460	613378	0.40
GY1149	NT	319531	603786	0.35

Sample No.	Square	Easting	Northing	IC
RJM719	NT	324000	600390	0.33
RJM720	NT	323120	600220	0.31
RJM721	NT	322500	601100	0.30
RJM722	NT	321000	602500	0.23
RJM723	NT	319210	604320	0.26
RJM724	NT	318910	605270	0.37
RJM735	NT	318090	622130	0.32
RJM736	NT	318610	622310	0.34
RJM737	NT	319620	623030	0.34
RJM738	NT	320260	623070	0.30
RJM739	NT	324450	623180	0.36
RJM860	NT	318022	620437	0.35
RJM888	NT	318156	624961	0.24
RJM889	NT	318997	624184	0.24

3. Sheet 9E sample

Sample No.	Square	Easting	Northing	IC
BRS1000	NX	295270	598380	0.30

4. Sheet 10W samples

Sample No.	Square	Easting	Northing	IC
BRS1044	NY	299370	596490	0.67
BRS1045	NY	299370	596490	0.65
BRS1046	NY	301020	596550	0.46
BRS1061	NY	313100	596200	0.41
BRS1062	NY	314200	598030	0.31
BRS1068	NY	304600	596880	0.44
BRS1071	NY	307280	597400	0.41

Sample No.	Square	Easting	Northing	IC
BRS1072	NY	308600	598200	0.44
BRS1084	NY	317180	598890	0.30
BRS1088	NY	316530	598210	0.22
BRS1107	NY	302220	597630	0.59
BRS1108	NY	303810	597700	0.42
BRS1117	NY	312230	597800	0.32
RJM686	NY	312820	598640	0.35

4. Sheet 10E sample

Sample No.	Square	Easting	Northing	IC
BRS1083	NY	317350	596990	0.31

5. Sheet 15E samples

Sample No.	Square	Easting	Northing	IC
AX 2732	NS	296000	601700	0.31
GY1043	NS	298345	603525	0.29
GY1057	NS	298060	616120	0.23
HFB118	NS	296020	627660	0.30
HFB131	NS	297250	625930	0.34
HFB133	NS	296760	627060	0.32
HFB134	NS	296650	626300	0.40
HFB135	NS	296290	625190	0.30
HFB136	NS	294930	626230	0.35
HFB137	NS	297230	625010	0.27
HFB145	NS	298350	625600	0.31
HFB146	NS	298780	626410	0.36
HFB147	NS	297880	625720	0.32
HFB148	NS	295190	627460	0.27
HFB178	NS	292850	626370	0.30
HFB183	NS	293640	627210	0.47
HFB187	NS	294160	626670	0.39
HFB189	NS	294520	627300	0.25
HFB222	NS	297000	622930	0.33
HFB225	NS	297210	623850	0.33
HFB230	NS	296470	624200	0.42
HFB232	NS	298540	624320	0.41
HFB240	NS	295580	622670	0.43
HFB241	NS	295320	622020	0.25
HFB243	NS	297820	619320	0.22

Sample No.	Square	Easting	Northing	IC
HFB244	NS	296270	620800	0.34
HFB259	NS	295010	617300	0.23
HFB266	NS	295480	624530	0.38
RJM600	NX	297170	599310	0.77
RJM601	NS	297090	600530	0.32
RJM602	NS	296310	600190	0.29
RJM615	NS	296390	611900	0.33
RJM616	NS	296300	610720	0.20
RJM617	NS	298000	609200	0.24
RJM619	NS	296720	609020	0.22
RJM620	NS	296270	607720	0.22
RJM621	NS	295640	608880	0.41
RJM623	NS	295650	605030	0.21
RJM627	NS	295520	602300	0.25
RJM628	NS	296180	604310	0.25
RJM629	NS	295490	615300	0.28
RJM641	NS	295700	617780	0.23
RJM642	NS	296130	616970	0.22
RJM643	NS	298030	616100	0.28
RJM680	NS	297910	611350	0.26
RJM681	NS	295580	606680	0.21
RJM691	NS	296300	614450	0.44
RJM692	NS	296850	613400	0.25
RJM693	NS	297000	614500	0.25
RJM694	NS	296700	614900	0.26

6. Sheet 23E samples

Sample No.	Square	Easting	Northing	IC
HFB 110	NS	296740	629610	0.42
HFB 114	NS	297450	628440	0.35
HFB 117	NS	296560	628820	0.57
HFB 119	NS	295300	628100	0.27
HFB 121	NS	298560	629120	0.34

Sample No.	Square	Easting	Northing	IC
HFB 122	NS	298740	629630	0.36
HFB 124	NS	298830	630060	0.4
HFB 127	NS	294930	628190	0.43
HFB 128	NS	297190	630270	0.56
HFB 149	NS	295120	628940	0.66

7. Sheet 24W samples

Sample No.	Square	Easting	Northing	IC
HFB 120	NS	299360	628560	0.36
HFB 126	NS	299950	630090	0.33
HFB 129	NS	299250	630950	0.74
HFB 130	NS	299930	631700	0.54
RJM1013	NT	307839	630774	0.38
RJM1056	NT	301906	630606	0.42
RJM1057	NT	301082	628221	0.32
RJM1060	NT	303240	629035	0.39
RJM1061	NT	303184	629780	0.36

Sample No.	Square	Easting	Northing	IC
RJM732	NT	312130	630820	0.21
RJM861	NT	315445	627522	0.21
RJM862	NT	315734	628378	0.24
RJM863	NT	313616	628509	0.25
RJM884	NT	303378	628761	0.27
RJM885	NT	302823	633293	0.50
RJM886	NT	307183	628201	0.30
RJM887	NT	306470	628710	0.29

8. Sheet 24E samples

Sample No.	Square	Easting	Northing	IC
BRS980	NT	320460	631040	0.29

Sample No.	Square	Easting	Northing	IC
BRS1153	NT	318400	630450	0.23